Modal Field Analysis of Meanderline Polarizer with Finite Thickness

#Chan Kwok Kee [1], Chio Tan Huat [2], Yeo Tat Soon [3]
[1]*Chan Technologies Inc.*
15 Links Lane, Brampton, Ontario L6Y 5H1, Canada
Email: kwok-kee.chan@rogers.com
[2]*DSO National Laboratories*
20 Science Park Drive, Singapore 118230
[3]*Temasek Defence Science Institute*
Block E1 #05-05, 1 Engineering Drive 2, Singapore 117576

Abstract

Most of the existing methods for the analysis of meanderline polarizer assume that the embedded metallic grids are infinitely thin. A new procedure is presented here for treating meanderline grids with finite thickness. The space between the metallic grids in a unit cell is considered as a meanderline waveguide with a stepped cross-section and length given by the grid thickness. The modes of this guide are obtained using the transverse resonance technique. A generalized scattering matrix characterization of the grid is obtained by field matching of the modes of the meanderline guide and the free space Floquet guide. The accuracy of this approach is verified by the very good agreement obtained between predicted and measured transmission phases of polarizer grids.

1. INTRODUCTION

The 90° meanderline polarizer is a very useful external means for converting an incident linear polarized plane wave into a circular polarized wave. The polarizing grid is doubly periodic and its configuration in a unit cell is shown in Fig. 1. In the following development, we will deal with a grid under normal incidence where the incident wave has its electric vector oriented in the 45° plane. This incident wave may be resolved into the two component TE_{00} and TM_{00} waves. For the former, the grid is normal to its electric vector and therefore appears to be capacitive. For the latter, the grid is parallel to the electric vector and hence is inductive to the incident wave. With the appropriate parameters and number of grid layers, a 90° phase differential can be created and approximately maintained between the TE_{00} and TM_{00} waves over a very broadband.

All existing methods for the analysis and design of the meanderline polarizer may be classified into two groups. The first group [1] makes use of equivalent network models of the grids and dielectric layers as well as transmission line theory to predict the polarizer performance. A number of iterations consisting of model adjustments, fabrication and test are required to arrive at satisfactory design. The second group [2, 3, 4] makes use of the Floquet Mode Expansion Moment Method to solve for the currents on the metallic grid, thereby giving the scattered fields. An integral equation of the grid currents is formulated by enforcing the continuity of the electric fields and discontinuity of the magnetic fields caused by the currents. In both groups, the metallic grid is assumed to be infinitely thin, which is essential for the second group. If the metallization is electrically thick, for instance, in a free-standing grid or at the higher frequencies or from the use of heavy metal cladding, the electrical performance obtained will be in error. This is typically manifested as a frequency shift of the electrical response. Until now, the grid thickness cannot be used as a design parameter. To account for the thickness of the metal, we propose a new method which solves for the fields in between the grids, rather than for the grid currents. It also has the advantage of using much fewer Floquet modes in the field expansion.

As shown in Fig. 1, the space in between two parallel grids in a unit cell is labelled here as a meanderline guide (MLG). Under normal incidence, the guide is symmetric about the centre wall (CW). The top (TW) and bottom (BW) walls of the guide are perfect electric conductors. Under normal TE incidence, the left (LW) and right (RW) walls as well as CW are perfect magnetic conductors (PMC). Under normal TM incidence, LW, RW and CW are perfect electric conductors (PEC). For the MLG with magnetic sidewalls, we need to find the TEM, TE and TM modes. For the MLG with electric sidewalls, TE and TM modes need to be determined. These modes are found using the Transverse Resonance Technique. Field matching between the MLG modes and the Floquet modes gives the Generalized Scattering Matrix (GSM) of the grid – free-space discontinuity. Combining these GSMs back-to-back together with that of the intervening guide to account for the metal thickness, results in the GSM of a thick polarizer screen.

2. MODES OF A MEANDERLINE GUIDE

Since the guide is symmetric about CW, we only need to develop the field representations in region I, II and III for each mode.

A. TEM Mode

The scalar potential satisfies Laplace equation and the pertinent field components are listed below. *L*, *M* and *N* terms are used to represent the field distributions in the three regions.

Region *I*:

$$E_x^I = -\sqrt{\eta_0}\left[\sum_{l=1,2,}^{L} A_l\left(\frac{l\pi}{d_1}\right)\sin\left(\frac{l\pi y}{d_1}\right)\sinh\left(\frac{l\pi x}{d_1}\right)\right]$$

$$E_y^I = \sqrt{\eta_0}\left[-\frac{1}{d_1} - \sum_{l=1,2,}^{L} A_l\left(\frac{l\pi}{d_1}\right)\cos\left(\frac{l\pi y}{d_1}\right)\cosh\left(\frac{l\pi x}{d_1}\right)\right]$$

$$H_x^I = \frac{1}{\sqrt{\eta_0}}\left[\frac{1}{d_1} + \sum_{l=1,2,}^{L} A_l\left(\frac{l\pi}{d_1}\right)\cos\left(\frac{l\pi y}{d_1}\right)\cosh\left(\frac{l\pi x}{d_1}\right)\right]$$

$$H_y^I = \frac{1}{\sqrt{\eta_0}}\left[-\sum_{l=1,2,}^{L} A_l\left(\frac{l\pi}{d_1}\right)\sin\left(\frac{l\pi y}{d_1}\right)\sinh\left(\frac{l\pi x}{d_1}\right)\right] \qquad (1)$$

Region *II*:

$$E_x^{II} = -\sqrt{\eta_0}\left\{\sum_{m=1,2,}^{M}\left(\frac{m\pi}{d_2}\right)\sin\left(\frac{m\pi}{d_2}(y-h)\right)\left[\begin{array}{l} B_m\cosh\left(\frac{m\pi}{d_2}(x-w_1)\right)+ \\ F_m\sinh\left(\frac{m\pi}{d_2}(x-w_1)\right)\end{array}\right]\right\}$$

$$E_y^{II} = \sqrt{\eta_0}\left\{-\frac{1}{d_2} - \sum_{m=1,2,}^{M}\left(\frac{m\pi}{d_2}\right)\cos\left(\frac{m\pi}{d_2}(y-h)\right)\left[\begin{array}{l} B_m\sinh\left(\frac{m\pi}{d_2}(x-w_1)\right)+ \\ F_m\cosh\left(\frac{m\pi}{d_2}(x-w_1)\right)\end{array}\right]\right\}$$

$$H_x^{II} = \frac{1}{\sqrt{\eta_0}}\left\{\frac{1}{d_2} + \sum_{m=1,2,}^{M}\left(\frac{m\pi}{d_2}\right)\cos\left(\frac{m\pi}{d_2}(y-h)\right)\left[\begin{array}{l} B_m\sinh\left(\frac{m\pi}{d_2}(x-w_1)\right)+ \\ F_m\cosh\left(\frac{m\pi}{d_2}(x-w_1)\right)\end{array}\right]\right\}$$

$$H_y^{II} = \frac{1}{\sqrt{\eta_0}}\left\{\sum_{m=1,2,}^{M}\left(\frac{m\pi}{d_2}\right)\sin\left(\frac{m\pi}{d_2}(y-h)\right)\left[\begin{array}{l} B_m\cosh\left(\frac{m\pi}{d_2}(x-w_1)\right)+ \\ F_m\sinh\left(\frac{m\pi}{d_2}(x-w_1)\right)\end{array}\right]\right\} \qquad (2)$$

Region *III*:

$$E_x^{III} = -\sqrt{\eta_0}\left[\sum_{n=1,2,}^{N} D_n\left(\frac{n\pi}{d_3}\right)\sin\left(\frac{n\pi}{d_3}(y-h)\right)\sinh\left(\frac{n\pi}{d_3}(x-\frac{T_x}{2})\right)\right]$$

$$E_y^{III} = \sqrt{\eta_0}\left[\frac{-1}{d_3} + \sum_{n=1,2,}^{N} D_n\left(\frac{n\pi}{d_3}\right)\cos\left(\frac{n\pi}{d_3}(y-h)\right)\cosh\left(\frac{n\pi}{d_3}(x-\frac{T_x}{2})\right)\right]$$

$$H_x^{III} = \frac{1}{\sqrt{\eta_0}}\left[\frac{1}{d_3} - \sum_{n=1,2,}^{N} D_n\left(\frac{n\pi}{d_3}\right)\cos\left(\frac{n\pi}{d_3}(y-h)\right)\cosh\left(\frac{n\pi}{d_3}(x-\frac{T_x}{2})\right)\right]$$

$$H_y^{III} = \frac{1}{\sqrt{\eta_0}}\left[\sum_{n=1,2,}^{N} D_n\left(\frac{n\pi}{d_3}\right)\sin\left(\frac{n\pi}{d_3}(y-h)\right)\sinh\left(\frac{n\pi}{d_3}(x-\frac{T_x}{2})\right)\right] \qquad (3)$$

The unknown coefficients [*A*], [*B*], [*D*] and [*F*] are found by matching E_y and H_y at $x = w_1$ and $x = w_1 + w_2$, the boundary between region *I* & *II* and region *II* & *III*. First solve for [*A*] using the following equation.

$$\left\{\left[C^I\right] + \left[Q^{II}\right][\gamma]^{-1}[\delta]\left[R^{II}\right]^T\left[S^I\right]\right\}[A] = \left[G^{II}\right] - \left[Q^{II}\right][\gamma]^{-1}\left[R^{III}\right]\left[S^{III}\right]\left[C^{III}\right]^{-1}\left[G^{III}\right] \qquad (4)$$

Then obtain the rest from

$$[B] = \left[R^{II}\right]^T\left[S^I\right][A] \qquad (5)$$

$$[F] = -[\gamma]^{-1}\left\{\left[R^{III}\right]\left[S^{III}\right]\left[C^{III}\right]^{-1}\left[G^{III}\right] + [\delta]\left[R^{II}\right]^T\left[S^I\right][A]\right\}$$

$$[D] = -\left[C^{III}\right]^{-1}\left\{\left[G^{III}\right] + \left[Q^{III}\right]^T\left[S^{II}\right][B] + \left[Q^{III}\right]^T\left[C^{II}\right][F]\right\}$$

where

$$[\gamma] = \left[S^{II}\right] + \left[R^{III}\right]\left[S^{III}\right]\left[C^{III}\right]^{-1}\left[Q^{III}\right]^T\left[C^{II}\right]$$

$$[\delta] = \left[C^{II}\right] + \left[R^{III}\right]\left[S^{III}\right]\left[C^{III}\right]^{-1}\left[Q^{III}\right]^T\left[S^{II}\right]$$

$\left[Q^{II}\right]$ = *L* × *M matrix with elements*

$$Q_{l,m}^{II} = \frac{m\pi}{d_2}\int_h^{h+d_2}\cos\left[\frac{m\pi}{d_2}(y-h)\right]\cos\left(\frac{l\pi y}{d_1}\right)dy$$

$\left[R^{II}\right]$ = *L* × *M matrix with elements*

$$R_{l,m}^{II} = \frac{2}{d_1}\frac{2}{m\pi}\int_h^{h+d_2}\sin\left[\frac{m\pi}{d_2}(y-h)\right]\sin\left(\frac{l\pi y}{d_1}\right)dy$$

$\left[Q^{III}\right]$ = *M* × *N matrix with elements*

$$Q_{m,n}^{III} = \frac{2}{d_2}\int_0^{d_2}\cos\left(\frac{m\pi y}{d_2}\right)\cos\left(\frac{n\pi y}{d_3}\right)dy$$

$\left[R^{III}\right]$ = *M* × *N matrix with elements*

$$R_{m,n}^{III} = \frac{2}{d_3}\int_0^{d_2}\sin\left(\frac{m\pi y}{d_2}\right)\sin\left(\frac{n\pi y}{d_3}\right)dy$$

$\left[G^{II}\right] = L \times 1$ *column matrix with elements*

$$G_l^{II} = \frac{1}{d_2}\int_h^{h+d_2} \cos\left(\frac{l\pi y}{d_1}\right) dy$$

$\left[G^{III}\right] = N \times 1$ *column matrix with elements*

$$G_n^{III} = \frac{1}{d_2}\int_0^{d_2} \cos\left(\frac{n\pi y}{d_3}\right) dy$$

$\left[C^{I}\right] = L\times L$ *diagonal matrix with* $C_{l,l}^{I} = \frac{l\pi}{2}\cosh\left(\frac{l\pi w_1}{d_1}\right)$

$\left[S^{I}\right] = L\times L$ *diagonal matrix with* $S_{l,l}^{I} = \frac{l\pi}{2}\sinh\left(\frac{l\pi w_1}{d_1}\right)$

$\left[C^{II}\right] = M\times M$ *diagonal matrix with* $C_{m,m}^{II} = \frac{m\pi}{2}\cosh\left(\frac{m\pi w_2}{d_2}\right)$

$\left[S^{II}\right] = M\times M$ *diagonal matrix with* $S_{m,m}^{II} = \frac{m\pi}{2}\sinh\left(\frac{m\pi w_2}{d_2}\right)$

$\left[C^{III}\right] = N\times N$ *diagonal matrix with* $C_{n,n}^{III} = \frac{n\pi}{2}\cosh\left(\frac{n\pi w_3}{d_3}\right)$

$\left[S^{III}\right] = N\times N$ *diagonal matrix with* $S_{n,n}^{III} = \frac{n\pi}{2}\sinh\left(\frac{n\pi w_3}{d_3}\right)$

The A, B, F and D coefficients of expansion need to be normalized by $(N^e)^{-1/2}$ so that power propagating through the MLG is unity.

$$N^e = \frac{2w_1}{d_1} + \frac{2w_2}{d_2} + \frac{2w_3}{d_3} + \sum_{l=1,2,}^{L} A_l^2\left(\frac{l\pi}{2}\right)\sinh\left(\frac{l\pi 2w_1}{d_1}\right) +$$

$$\sum_{m=1,2,}^{M} (m\pi)\sinh\left(\frac{m\pi}{d_2}w_2\right)\left\{\begin{array}{l}\left[B_m^2 + C_m^2\right]\cosh\left(\frac{m\pi}{d_2}w_2\right) + \\ 2B_m C_m \sinh\left(\frac{m\pi}{d_2}w_2\right)\end{array}\right\} +$$

$$\sum_{n=1,2,}^{N} D_n^2\left(\frac{n\pi}{2}\right)\sinh\left(\frac{n\pi 2w_3}{d_3}\right) \qquad (6)$$

B. TE_z Modes

The cross section of the MLG needs to be characterized by its S-matrix in the transverse X-direction so that the boundary condition at the sidewalls may be applied to achieve the transverse resonance condition. To this end, we first characterize the discontinuity between region I and II as shown in Fig. 2.

Region *I*:
The scalar potential for this region may be written as

$$\psi^I = \sum_{l=0,1,}^{L-1}\left[-a_l^I e^{-jk_{xl}^I x'} + b_l^I e^{+jk_{xl}^I x'}\right]\cos\left(\frac{l\pi y'}{d_1}\right)e^{-jk_z z'}$$

where a_l^I and b_l^I represent the incident and reflected waves of region I. The origin of the (x', y', z') coordinate system is located at the (x=w_1,y=0,z=0). The field components are as follows.

$$E_x = \sum_{l=0,1,}^{L-1}\left[-a_l^I e^{-jk_{xl}^I x'} + b_l^I e^{+jk_{xl}^I x'}\right]\frac{l\pi}{d_1}\sin\left(\frac{l\pi y'}{d_1}\right)e^{-jk_z z'}$$

$$E_y = \sum_{l=0,1,}^{L-1}\left[a_l^I e^{-jk_{xl}^I x'} + b_l^I e^{+jk_{xl}^I x'}\right]\cos\left(\frac{l\pi y'}{d_1}\right)jk_{xl}^I e^{-jk_z z'}$$

$$H_x = \frac{-k_z}{\omega\mu}\sum_{l=0,1,}^{L-1}\left[a_l^I e^{-jk_{xl}^I x'} + b_l^I e^{+jk_{xl}^I x'}\right]jk_{xl}^I\cos\left(\frac{l\pi y'}{d_1}\right)e^{-jk_z z'}$$

$$H_y = \frac{k_z}{\omega\mu}\sum_{l=0,1,}^{L-1}\left[-a_l^I e^{-jk_{xl}^I x'} + b_l^I e^{+jk_{xl}^I x'}\right]\frac{l\pi}{d_1}\sin\left(\frac{l\pi y'}{d_1}\right)e^{-jk_z z'}$$

$$H_z = \frac{k_c^2}{j\omega\mu}\sum_{l=0,1,}^{L-1}\left[-a_l^I e^{-jk_{xl}^I x'} + b_l^I e^{+jk_{xl}^I x'}\right]\cos\left(\frac{l\pi y'}{d_1}\right)e^{-jk_z z'}$$

$$k_{xl}^I = \sqrt{k_c^2 - \left(\frac{l\pi}{d_1}\right)^2} \qquad (7)$$

Region *II*:
The scalar potential for this region may be written as

$$\psi^{II} = \sum_{m=0,1,}^{M-1}\left[a_m^{II} e^{+jk_{xm}^{II} x'} - b_m^{II} e^{-jk_{xm}^{II} x'}\right]\cos\left(\frac{m\pi}{d_2}(y'-h)\right)e^{-jk_z z'}$$

where a_m^{II} and b_m^{II} represent the incident and reflected waves of region *II*. The E_y and H_z field components are

$$E_x = \sum_{m=0,1,}^{M-1}\left[a_m^{II} e^{+jk_{xm}^{II} x'} - b_m^{II} e^{-jk_{xm}^{II} x'}\right]\frac{m\pi}{d_2}\sin\left(\frac{m\pi}{d_2}(y'-h)\right)e^{-jk_z z'}$$

$$E_y = \sum_{m=0,1,}^{M-1}\left[a_m^{II} e^{+jk_{xm}^{II} x'} + b_m^{II} e^{-jk_{xm}^{II} x'}\right]\cos\left(\frac{m\pi}{d_2}(y'-h)\right)jk_{xm}^{II} e^{-jk_z z'}$$

$$H_x = \frac{-k_z}{\omega\mu}\sum_{m=0,1,}^{M-1}\left[a_m^{II} e^{+jk_{xm}^{II} x'} + b_m^{II} e^{-jk_{xm}^{II} x'}\right]\cos\left(\frac{m\pi}{d_2}(y'-h)\right)jk_{xm}^{II} \cdot e^{-jk_z z'}$$

$$H_y = \frac{k_z}{\omega\mu}\sum_{m=0,1,}^{M-1}\left[a_m^{II} e^{+jk_{xm}^{II} x'} - b_m^{II} e^{-jk_{xm}^{II} x'}\right]\frac{m\pi}{d_2}\sin\left(\frac{m\pi}{d_2}(y'-h)\right) \cdot e^{-jk_z z'}$$

$$H_z = \frac{k_c^2}{j\omega\mu}\sum_{m=0,1,}^{M-1}\left[a_m^{II} e^{+jk_{xm}^{II} x'} - b_m^{II} e^{-jk_{xm}^{II} x'}\right]\cos\left(\frac{m\pi}{d_2}(y'-h)\right)e^{-jk_z z'}$$

$$k_{xm}^{II} = \sqrt{k_c^2 - \left(\frac{m\pi}{d_2}\right)^2} \qquad (8)$$

Match E_y of region I and II at x' = 0, form the inner product of the resulting equation with cos ($i\pi y/d_1$) and integrate from y=h to y=h+d_2. Similarly, match H_z of region I and II at x' =

0, form the inner product with cos $[i\pi(y-h)/d_2]$ and integrate from y=h to y=h+d_2. We end up with the following S-matrix description of the step-down junction.

$$[S_{11}] = \left\{[I] + [P][Q]^T\right\}^{-1} \left\{[P][Q]^T - [I]\right\}$$

$$[S_{12}] = 2\left\{[I] + [P][Q]^T\right\}^{-1}[P] = [P] - [S_{11}][P]$$

$$[S_{21}] = [Q]^T\left\{[I] - [S_{11}]\right\}$$

$$[S_{22}] = [U] - [Q]^T[S_{12}] \qquad (9)$$

The matrices of the above equation are defined as follows.

$$[P] = \left[K^I\right]^{-1}[Q]\left[K^{II}\right]$$

$[Q] = L \times M$ *matrix with elements*

$$Q_{l,m} = \frac{2}{\varepsilon_l d_2}\int_h^{h+d_2} \cos\left[\frac{m\pi}{d_2}(y-h)\right]\cos\left(\frac{l\pi y}{d_1}\right)dy$$

$\varepsilon_l = 2$, *if* $l = 0$

$= 1$, *if* $l \neq 0$

$\left[K^I\right] = L \times L$ *diagonal matrix with element* $K^I_{l,l} = K^I_{xl}\, d_1$

$\left[K^{II}\right] = M \times M$ *diagonal matrix with element* $K^{II}_{m,m} = K^{II}_{xm}\, d_2$

$[I] = L \times L$ *unit matrix*

$[U] = M \times M$ *unit matrix*

Elements of the Q, P and K matrices can be evaluated in closed form so that the S-matrix of the junction is readily obtained. The S-matrix of the junction between region II and III is similarly found by substituting in the appropriate parameters. The S-matrices of the two step junctions can now be combined together with those of the uniform guide sections of region *I*, *II* and *III* to give an overall S-matrix description, S^M, of the symmetric half of the MLG. If boundary condition (BC) is imposed on the sidewalls LW and CW, we end up with the following characteristic matrix equation

$$\begin{pmatrix} \left[S^M_{11}\right] - \left[D^L\right] & \left[S^M_{12}\right] \\ \left[S^M_{21}\right] & \left[S^M_{22}\right] - \left[D^C\right] \end{pmatrix} \begin{pmatrix} \left[a^L\right] \\ \left[a^C\right] \end{pmatrix} = \begin{pmatrix} [0] \\ [0] \end{pmatrix} \qquad (10)$$

$[D^L]$ is a diagonal matrix with coefficient of +1 if LW is a PMC and -1 if LW is a PEC. Similarly for $[D^C]$ expressing the BC for CW. $[a^L]$ and $[a^C]$ are the incident waves at LW and CW respectively. For a non-trivial solution, the determinant of equation (10) vanishes at the mode cutoff wave numbers, k_c.

The bracketing and bisection method is used to find the roots, k_c, of the matrix determinant. For a given root, the first unknown variable of the column matrix $[a^L]$ is set to 1. The first column of the characteristic equation can then be transferred over to the right hand side so that the equation may be written as [S'][a']=[b']. The remaining incident wave variables can now be determined through the least squares approach by multiplying both sides with the conjugate transpose of the LHS coefficient matrix $[S']^\dagger[S'][a'] = [S']^\dagger[b']$. Once the incident and reflected wave variables are determined in all regions of the MLG cross-section, they are normalized by the square root of the mode power transmitted by the MLG.

C. TM$_z$ Modes

Region *I*:
The scalar potential for this region may be written as

$$\psi^I_e = \sum_{l=1,2,}^{L}\left[a^I_{el}\, e^{-jk^I_{xel}x'} + b^I_{el}\, e^{+jk^I_{xel}x'}\right]\sin\left(\frac{l\pi y'}{d_1}\right)e^{-jk_{ze}z'}$$

where $a_{el}{}^I$ and $b_{el}{}^I$ represent the incident and reflected waves of region *I*. The origin of the (x', y', z') coordinate system is located at the ($x=w_1$, y=0, z=0).

$$E_x = \frac{k_{ze}}{\omega\varepsilon}\sum_{l=1,2,}^{L}\left[a^I_{el}\, e^{-jk^I_{xel}x'} - b^I_{el}\, e^{+jk^I_{xel}x'}\right]\left(jk^I_{xel}\right)\sin\left(\frac{l\pi y'}{d_1}\right)e^{-jk_{ze}z'}$$

$$E_y = \frac{-k_{ze}}{\omega\varepsilon}\sum_{l=1,2,}^{L}\left[a^I_{el}\, e^{-jk^I_{xel}x'} + b^I_{el}\, e^{+jk^I_{xel}x'}\right]\left(\frac{l\pi}{d_1}\right)\cos\left(\frac{l\pi y'}{d_1}\right)e^{-jk_{ze}z'}$$

$$E_z = \frac{k^2_{ce}}{j\omega\varepsilon}\sum_{l=1,2,}^{L}\left[a^I_{el}\, e^{-jk^I_{xel}x'} + b^I_{el}\, e^{+jk^I_{xel}x'}\right]\sin\left(\frac{l\pi y'}{d_1}\right)e^{-jk_{ze}z'}$$

$$H_x = \sum_{l=1,2,}^{L}\left[a^I_{el}\, e^{-jk^I_{xel}x'} + b^I_{el}\, e^{+jk^I_{xel}x'}\right]\left(\frac{l\pi}{d_1}\right)\cos\left(\frac{l\pi y'}{d_1}\right)e^{-jk_{ze}z'}$$

$$H_y = \sum_{l=1,2,}^{L}\left[a^I_{el}\, e^{-jk^I_{xel}x'} - b^I_{el}\, e^{+jk^I_{xel}x'}\right]jk^I_{xel}\,\sin\left(\frac{l\pi y'}{d_1}\right)e^{-jk_{ze}z'}$$

$$k^I_{xel} = \sqrt{(k_{ce})^2 - \left(\frac{l\pi}{d_1}\right)^2} \qquad (11)$$

Region *II*:
The scalar potential for this region may be written as

$$\psi^{II}_e = \sum_{m=1,2,}^{M}\left[a^{II}_{em}\, e^{+jk^{II}_{xem}x'} + b^{II}_{em}\, e^{-jk^{II}_{xem}x'}\right]\sin\left(\frac{m\pi}{d_2}(y'-h)\right)e^{-jk_{ze}z'}$$

where $a_{em}{}^{II}$ and $b_{em}{}^{II}$ represent the incident and reflected waves of region *II*. The field components are

$$E_x = \frac{k_{ze}}{\omega\varepsilon}\sum_{m=1,2,}^{M}\left[-a^{II}_{em}\, e^{+jk^{II}_{xem}x'} + b^{II}_{em}\, e^{-jk^{II}_{xem}x'}\right]jk^{II}_{xem}\sin\left[\frac{m\pi(y'-h)}{d_2}\right] \cdot e^{-jk_{ze}z'}$$

$$E_y = \frac{-k_{ze}}{\omega\varepsilon}\sum_{m=1,2,}^{M}\left[a^{II}_{em}\, e^{+jk^{II}_{xem}x'} + b^{II}_{em}\, e^{-jk^{II}_{xem}x'}\right]\frac{m\pi}{d_2}\cos\left[\frac{m\pi(y'-h)}{d_2}\right] \cdot e^{-jk_{ze}z'}$$

$$E_z = \frac{k^2_{ce}}{j\omega\varepsilon}\sum_{m=1,2,}^{M}\left[a^{II}_{em}\, e^{+jk^{II}_{xm}x'} + b^{II}_{em}\, e^{-jk^{II}_{xm}x'}\right]\sin\left(\frac{m\pi}{d_2}(y'-h)\right)e^{-jk_{ze}z'}$$

$$H_x = \sum_{m=1,2,}^{M} \left[a_{em}^{II} e^{+jk_{xem}^{II} x'} + b_{em}^{II} e^{-jk_{xem}^{II} x'} \right] \frac{m\pi}{d_2} cos\left[\frac{m\pi(y'-h)}{d_2} \right] \cdot e^{-jk_{ze} z'}$$

$$H_y = \sum_{m=1,2,}^{M} \left[-a_{em}^{II} e^{+jk_{xem}^{II} x'} + b_{em}^{II} e^{-jk_{xem}^{II} x'} \right] jk_{xem}^{II} sin\left[\frac{m\pi(y'-h)}{d_2} \right] \cdot e^{-jk_{ze} z'}$$

$$k_{xem}^{II} = \sqrt{k_{ce}^2 - \left(\frac{m\pi}{d_2} \right)^2} \qquad (12)$$

Match E_z of region I and II at x' = 0, form the inner product of the resulting equation with sin ($i\pi y/d_1$) and integrate from y=h to y=h+d_2. Similarly, match H_y of region I and II at x' = 0, form the inner product with sin [$i\pi(y - h)/d_2$)] and integrate from y=h to y=h+d_2. We end up with the following S-matrix description of the step-down junction.

$$[S_{11}] = \{[I] + [q][p]\}^{-1} \{[q][p] - [I]\}$$
$$[S_{12}] = [q] - [S_{11}][q]$$
$$[S_{21}] = [p]\{[I] - [S_{11}]\}$$
$$[S_{22}] = [U] - [S_{21}][q] \qquad (13)$$

The matrices of the above equation are defined as follows.

$$[p] = \left[K_e^{II}\right]^{-1} [q]^T \left[K_e^I\right]$$

$[q] = L \times M$ *matrix with elements*

$$q_{l,m} = \frac{2}{d_1} \int_h^{h+d_2} sin\left[\frac{m\pi}{d_2}(y-h) \right] cos\left(\frac{l\pi y}{d_1} \right) dy$$

$\left[K_e^I\right] = L \times L$ *diagonal matrix with element* $= K_{xel}^I d_1 / 2$

$\left[K_e^{II}\right] = M \times M$ *diagonal matrix with element* $= K_{xem}^{II} d_2 / 2$

$[I] = L \times L$ *unit matrix*

$[U] = M \times M$ *unit matrix*

The mode characteristic matrix equation can now be set-up as for the TE_z case. The mode cutoff wave numbers and wave variables in the various regions are determined accordingly.

3. MEANDERLINE GUIDE – FREE SPACE JUNCTION

The S-matrix of the MLG – free space junction is given by eqn. (9) where the elements of the P and Q matrices are defined as follows.

$$P_{l,m} = \frac{\sqrt{\eta_m^{(mlg)}}}{\sqrt{\eta_l^{(fs)}}} \iint_{mlg} \left[\bar{e}_m^{(mlg)} \times \bar{h}_l^{(fs)} \right] \cdot \hat{z}\, dS$$

$$Q_{l,m} = \frac{\sqrt{\eta_m^{(mlg)}}}{\sqrt{\eta_l^{(fs)}}} \iint_{mlg} \left[\bar{e}_m^{(mlg)*} \times \bar{h}_l^{(fs)} \right] \cdot \hat{z}\, dS \qquad (14)$$

The Floquet mode index is *l* and MLG mode index is *m*. The mode impedance is given by η. These integrations of the MLG electric field mode vectors, $\bar{e}_m^{(mlg)}$, and the Floquet magnetic field mode vectors, $\bar{h}_l^{(fs)}$, can be done in closed form, leading to an efficient generation of the S-matrix.

4. RESULTS

The theoretical procedure presented here was verified by predicting the transmission phases of meanderline grids printed on a dielectric substrate as shown in Fig. 3. Effects of the dielectric support are included here by combining the GSM of the slab to that of the grid. The parameters and test results for two such grids were published by Terret et al [2]. However, no grid thickness was given, so 1-oz copper metallization is assumed for the computations carried out here. The transmission phases and the differential phase shift of the TE_{00} and TM_{00} modes for the two grids are plotted in Fig. 4 and 5. Details of the grids are given in the respective plots. The differences between the two grids are the width w and height h of the lines. For the field approximation, the minimum highest cutoff wave number required for the MLG modes to achieve convergence is approximately 90. This yields 44 modes for the Grid 'A' MLG with PMC sidewalls and 40 modes with PEC sidewalls. To generate these modes, the number of functions used in region I, II and III is L=13, M=9 and N=13 respectively. The highest cutoff wave number of the Floquet modes needed for convergence must be at least 15% larger so that 138 free space modes are used. The number of Floquet modes is significantly less, approximately 3 times less than that required for the grid current approach. Grid 'B' MLG has 44 modes with PMC sidewalls and 38 modes with PEC sidewalls. The number of expansion functions in the 3 regions is 13, 8 and 13. Both the transmission phases and differential phase shift show very good agreement with measurements for both grids across the frequency band. Only the measured differential phase shift is plotted here for comparison. In conclusion, a method has been developed that can analyse accurately meanderline grid with finite thickness.

REFERENCES

[1] R.S. Chu and K.M. Lee, "Analytical model of a multilayered meanderline polarizer plate with normal and oblique plane-wave incidence", IEEE AP-35, No. 6, 1987, pp. 652-661.

[2] C. Terret, J. Levrel and K. Mahdjoubi, "Susceptance computation of a meanderline polarizer layer", IEEE AP-32, No. 9, 1984, pp. 1007 – 1011.

[3] K. K. Chan, S. R. Gauthier and G. Dinham, "A broadband and wide angle meanderline polarizer", Proc. Of 3rd International Conf. On Electromagnetics in Aerospace Applications, Torino, Italy, Sept. 1993, pp. 171 - 174.

[4] R. A. Marino, "Accurate and efficient modelling of meanderline polarizers," Microwave Journal, Vol. 41, No. 11, Nov. 1998, pp. 22 - 34.

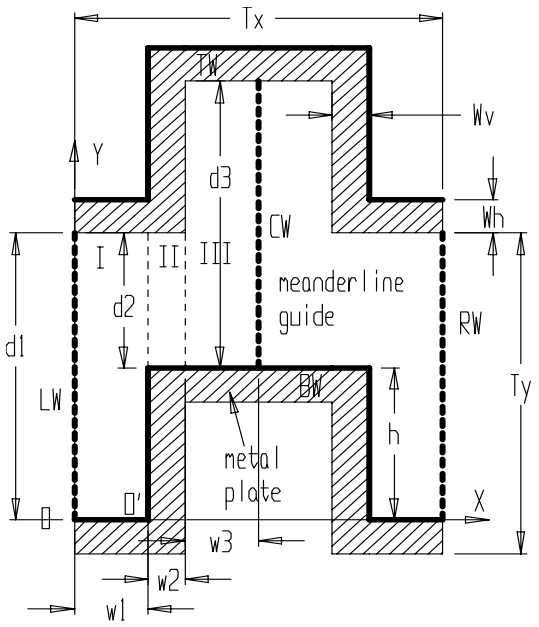

Fig. 1: Unit Cell of a Meanderline Polarizer.

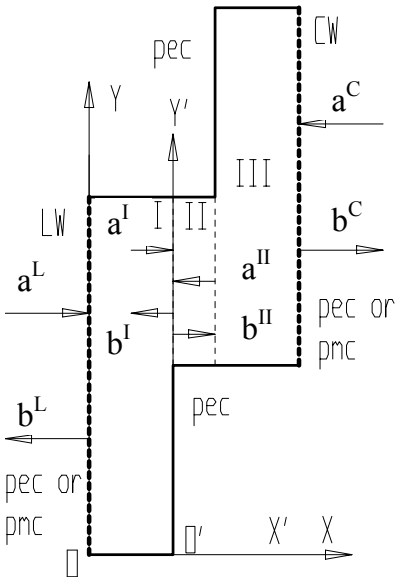

Fig. 2: Step Junctions of Symmetric Half of MLG

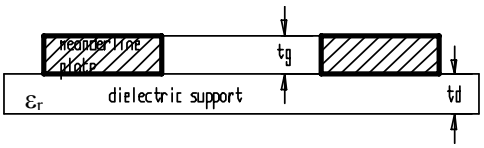

Fig. 3: Printed Meanderline Grid on a Dielectric Sheet

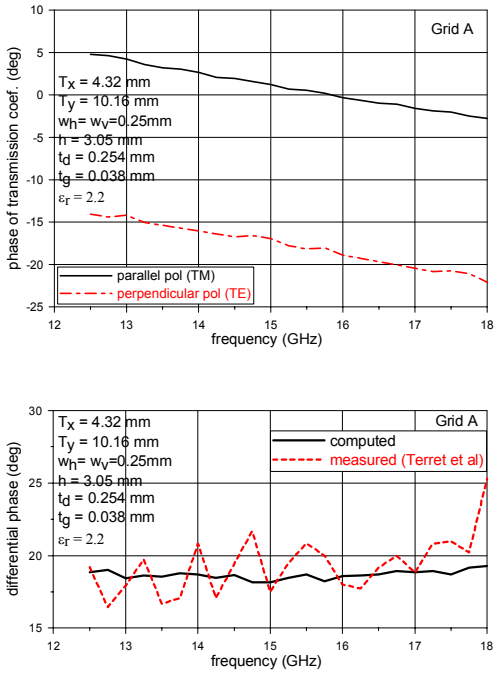

Fig. 4: Transmission Phases and Differential Phase Shift of TE_{00} and TM_{00} Modes for Grid A.

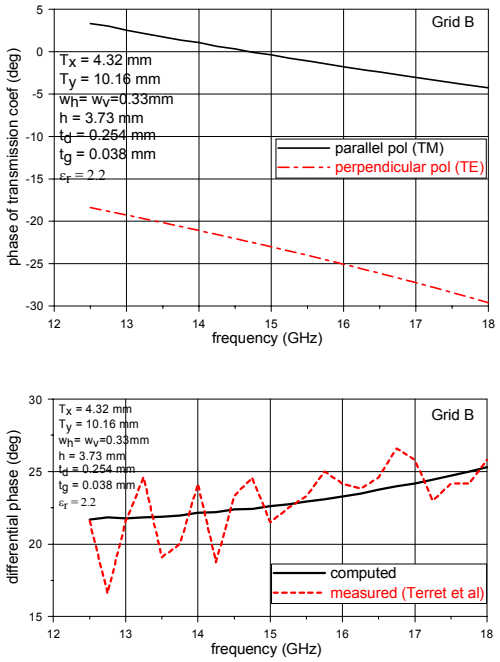

Fig. 5: Transmission Phases and Differential Phase Shift of TE_{00} and TM_{00} Modes for Grid B.